A&A 375, 492–497 (2001)
DOI: 10.1051/0004-6361:20010693

Astronomy & Astrophysics

The coronal FeXXI λ1354.094 line in AB Doradus⋆

O. Vilhu⋆⋆,[1], P. Muhli[1], R. Mewe[2], and P. Hakala[3]

[1] Observatory, Box 14, 00014 University of Helsinki, Finland
e-mail: vilhu@astro.helsinki.fi, muhli@astro.helsinki.fi
[2] SRON Laboratory for Space Research, Sorbonnelaan 2, 3584 CA Utrecht, The Netherlands
e-mail: R.Mewe@sron.nl
[3] Tuorla Observatory, University of Turku, Finland
e-mail: pahakala@astro.utu.fi

Received 10 April 2001 / Accepted 10 May 2001

Abstract. The active late-type star AB Doradus was observed in February 1996 with the Goddard High Resolution Spectrograph of the *Hubble Space Telescope* using the low resolution G140L grating. The observations covered one half of the star's rotation cycle ($P = 0.514$ d) with 11.5 min time resolution. The strong coronal FeXXI λ1354.094 line formed at 10^7 K was analysed and its emission measure (EM) derived. This EM is much higher than that derived from recent XMM-Newton observations (Güdel et al. 2001), and earlier EXOSAT (Collier Cameron et al. 1988) and ASCA/EUVE (Mewe et al. 1996) data, as well, requiring a variability by a factor of 5. The physical reason for the variability remains unknown, since (outside flares) the observed broad band variability of AB Dor is much smaller.

Key words. stars: coronae – stars: activity – stars: individual: AB Dor – ultraviolet: stars

1. Introduction

AB Doradus is a young and rapidly rotating late-type star (K1 IV, $P_{\rm rot} = 0.514$ d, $v \sin i = 100\,{\rm km\,s^{-1}}$) whose corona has been extensively studied due to its brightness and activity. The hot (10^{6-7} K) corona of AB Dor is best visible in the extreme ultraviolet (Rucinski et al. 1995, EUVE) and soft X-rays (Collier Cameron et al. 1988, EXOSAT; Vilhu et al. 1987, GINGA; Mewe et al. 1996, ASCA; Kürster at al. 1997, ROSAT; Güdel et al. 2001, XMM-Newton). In particular, XMM-Newton confirmed the low coronal iron abundance found by the EUVE/ASCA-combination (Mewe et al. 1996), which was 4–5 times lower than the photospheric abundance (Vilhu et al. 1987). Further, XMM-Newton, EUVE and ASCA have permitted very detailed studies of the coronal temperature stratification using lines formed at different temperatures.

A few weak coronal lines also exist at longer wavelengths. A potentially important case is FeXXI λ1354.094 which is an M1-type forbidden transition between two fine structure levels of the ground state of FeXXI. The line is optimally formed at 10^7 K and is accessible to the Hubble Space Telescope (HST) spectrographs. Using HST, the line was discovered in HR 1099 (Robinson et al. 1996), Capella (Linsky et al. 1998) and AU Mic (Pagano et al. 2000) giving an opportunity to study the whole chromospheric-coronal complex simultaneously using far ultraviolet lines only.

Using HST, we observed the FeXXI-line of AB Dor during half of its rotational period. We present the results and methods to analyse the line strength in terms of the emission measure.

2. Observations

The observations were performed with the *Goddard High Resolution Spectrograph* (GHRS) onboard the *Hubble Space Telescope* (HST) on February 5th, 1996. This was a repeat run of our original programme (ID 5310) which failed partially in November 1994. The target was in the Continuous Viewing Zone (CVZ), hence we were able to acquire a continuous series of spectra interrupted only by three South Atlantic Anomaly (SAA) passages. We used the G140L low-resolution grating which provides a resolving power $R = \lambda/\delta\lambda \approx 2100$ at the coronal FeXXI 1354 Å line, giving a spectral resolution of ∼150 km s^{-1}. The spectra which covered a wavelength range of ∼1290–1580 Å were captured with the D1 Digicon detector using the

Send offprint requests to: O. Vilhu,
e-mail: osmi.vilhu@helsinki.fi

⋆ Based on observations with the NASA/ESA *Hubble Space telescope*, obtained at the Space Telescope Science Institute, which is operated by the Association of Universities for Research in Astronomy, Inc., under the NASA contract NAS 5-26555.

⋆⋆ *Hubble Space Telescope* Guest Observer.

2.0 arcsec square Large Science Aperture (LSA). The science exposures were preceded by a Spectrum Y Balance (SPYBAL) calibration lamp exposure with a slightly different carrousel position for the G140L grating as compared to the subsequent target observations. However, we made use of the calibration spectrum to determine the zero-point offset of the default wavelength solution of the spectra, providing an adequately accurate wavelength calibration as to the low spectral resolution.

The science exposures, obtained at 03.796–09.943 (heliocentric) UT (about one half of the rotation period of our target) using the ACCUM mode, resulted in 32 spectra with 11.53 min average time resolution (including overheads and SAA passages). The default COMB = FOUR setting was used to compensate for diode response variations. The response irregularities due to photocathode granularity were not corrected for (FP-SPLIT = NO) and only the half-diode width subsampling method (STEP-PATT = 4) was implemented, since we desired to maximise the time resolution of our observations.

The spectra were reduced with the IRAF (Image Reduction and Analysis Facility) and STSDAS (Space Telescope Science Data Analysis System) software. Utilising the best calibration reference files available at the time of the reductions (February 1998) we used the *calhrs* calibration routine to assign wavelength solution, flux values and error estimates to the raw GHRS data. Furthermore, the wavelength scale of the science spectra was adjusted using the *waveoff* task and the SPYBAL calibration spectrum so that any zero-point offset from the default wavelength solution could be corrected for.

Figure 1 shows the average spectrum excluding the flare spectrum at phase 0.8 (see Fig. 3). The mean intensity $(1.25 \pm 0.05) \times 10^{-12}$ erg cm^{-2} s^{-1} of the strongest line, the CIV 1549 doublet, is very close to that observed one year earlier with HST (Vilhu et al. 1998; Brandt et al. 2001).

Figure 2 shows an enlargement of the FeXXI λ1354.094 region. For comparison, the solar-quiet network spectrum (multiplied by 10 and scaled to AB Dor's distance of 15 pc) as observed by SUMER on board SOHO (Curdt 1998; Wilhelm et al. 1999) is overplotted. The solar spectrum, broadened by the instrumental (150 km s^{-1}) and rotational (100 km s^{-1}) profiles, is also shown.

Figure 3 shows light curves of selected lines (marked in Fig. 1) using the canonical ephemeris (Innis et al. 1988):

$$\text{phase}(0.0) = \text{HJD } 2444296.575 + 0.51479E. \quad (1)$$

The flare at phase 0.8 did not produce apparently any hot optically thin gas since no trace of it is visible in the FeXXI 1354.094 line.

3. Calculation of the FeXXI λ1354.094 line strength

A multi-Gaussian fit was applied to the region of the spectrum shown in Fig. 2 resulting in the line parameters given in Table 1.

The coronal FeXXI 1354.094 line (Dere et al. 1997) is a blend with CI 1354.288 and cannot be separated with our resolution. Fortunately, there is another CI line nearby at 1364.164 which is stronger in the Sun (see the dotted line in Fig. 2) and Capella (Linsky et al. 1998) compared to the λ1354.288 line. Hence, we can safely assume that its contribution is also small in AB Dor. The blending with the nearby OI 1355.60 line can be resolved with Gaussian fits and the FeXXI line flux ($3.03 \pm 0.3 \times 10^{-14}$ erg cm^{-2}) properly estimated.

We calculate the line strength of the FeXXI λ1354.094 line which is an M1-type forbidden transition between two (of four total) fine structure levels (1–2) of the ground state ^{3}P. We follow the procedure given by Mewe et al. (1985).

The line strength (photons/cm^3/s) of a given transition from level j to level k (not necessarily the original level i from which the line was excited) is given by

$$P_{jk}^{\rm exc} = S_{\rm exc}\ BR\ n_{\rm e}\ N_{\rm ion}, \quad (2)$$

where $BR \equiv A_{jk}/\sum_{\ell \le j} A_{j\ell}$ is the branching ratio (the A's are radiative transition probabilities), $n_{\rm e}$ is the electron density (in cm^{-3}), $N_{\rm ion}$ is the concentration (in cm^{-3}) of the radiating ion, and $S_{\rm exc}$ is the electron collisional excitation rate coefficient (in cm^3 s^{-1}) given by

$$S_{\rm exc} = 8.63 \times 10^{-6} \left(\frac{\bar{\Omega}(y)}{w_i}\right) T^{-1/2} {\rm e}^{-y}, \quad (3)$$

where $y = E_{\rm exc}/kT = 1.43877 \times 10^8\ a/\lambda T$ (electron temperature T in K and wavelength λ in Å). Here $a = E_{\rm exc}/h\nu$, the ratio of line excitation and photon energy ($a > 1$ for a line transition not ending on the ground level). Further, $\bar{\Omega}(y)$ is the collision strength averaged over a Maxwellian electron energy distribution and w_i is the statistical weight of the initial lower (usually ground) level.

The reduced line strength P' in energy units of 10^{-23} erg cm^3 s^{-1} is given by

$$P' \equiv 10^{-Q} \equiv 10^{23} P/(n_{\rm e} N_{\rm H}), \quad (4)$$

or

$$P' = 10^{23} BR\ E_{\rm ph}\ S_{\rm exc}\ (N_{\rm ion}/N_{\rm el})(N_{\rm el}/N_{\rm H}), \quad (5)$$

where $E_{\rm ph}$ is the photon energy in ergs ($=1.9863 \times 10^{-8}/\lambda$(Å)), $N_{\rm ion}/N_{\rm el}$ is the ion fraction given by Arnaud & Rothenflug (1985, Ar-Ro) or Arnaud & Raymond (1992, Ar-Ra), $N_{\rm el}/N_{\rm H}$ is the iron abundance relative to Hydrogen and Q is the exponent given in the line flux Table IV of Mewe et al. (1985). We adopt 4.68×10^{-5} as the solar iron abundance relative to hydrogen (Anders & Grevesse 1989).

Substituting relevant data and rewriting, in this special case, gives:

$$P' = 253.7({\rm Fe/Fe}_\odot)\ \frac{BR\bar{\Omega}(y)}{\lambda w_i} \frac{N_{\rm ion}}{N_{\rm el}} \frac{1}{\sqrt{T}} {\rm e}^{-14.3877a/\lambda T}, \quad (6)$$

where T is in units of 10^7 K, λ in Å and Fe/Fe$_\odot$ is the coronal iron abundance relative to the solar photospheric

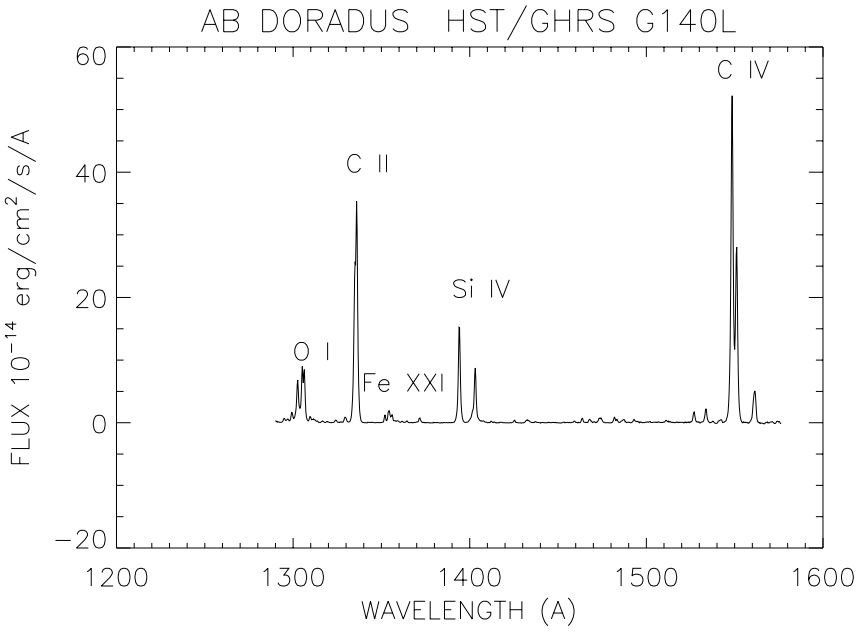

Fig. 1. The spectrum of AB Doradus as observed with the G140L grating of the Goddard High Resolution Spectrograph of the Hubble Space Telescope.

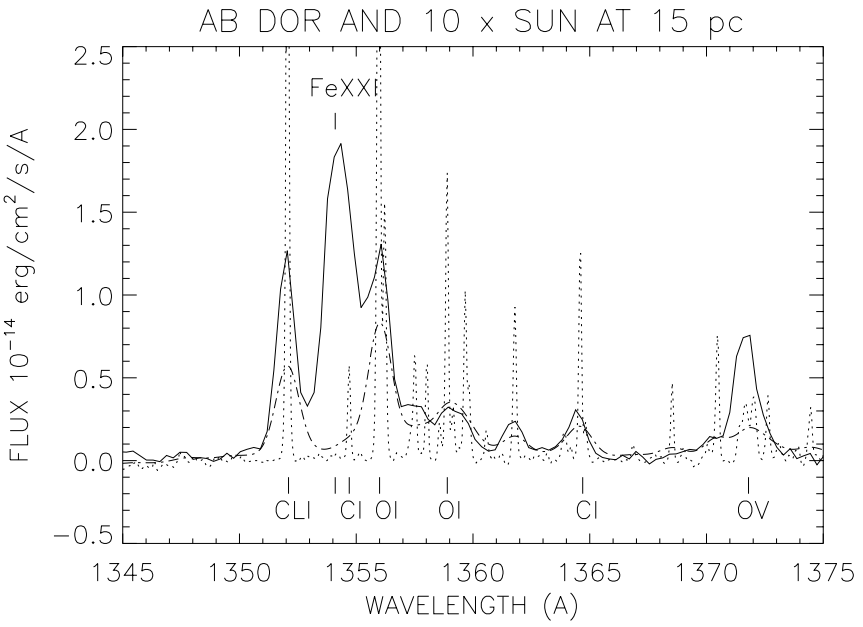

Fig. 2. An enlargement of the spectrum in Fig. 1 around the FeXXI λ1354.094 line (the solid line). A quiet network solar spectrum multiplied by 10 and scaled to a distance of 15 pc is also shown with and without instrumental (150 km s^{-1}) and rotational (90 km s^{-1}) broadening (dash-dot and dashed lines).

one. For transitions from the ground state $a = 1$ and $w_i = 1$ and for the λ1354 line we also have $BR = 1$. The collision strength $\bar{\Omega}(y)$ is taken from the calculations by Aggarwal (1991) who takes into account the effect of near-Threshold resonances.

Collisional depopulation of level 2 begins at an electron density (n_e) where $n_e S_{exc}$ exceeds A, i.e., at $n_e \sim 4 \times 10^{14}$ cm^{-3}, well above typical stellar coronal densities and we neglect these effects.

However, the excitations to neighbouring levels 1–3 and 1–4 also contribute nearly fully to the population of the upper level 2 of the 1354 line because the radiations from levels 3 and 4 ultimately cascade down to level 2. With the collision strengths from Aggarwal (1991) and branching ratios based on transition probabilities from the CHIANTI data base (Dere et al. 1997) we estimate that the cascades enhance the excitation rate 1–2 by a factor of $F \simeq 2$–2.2 which gives

$$P' \equiv 10^{-23}(\mathrm{Fe/Fe_\odot})10^{-Q^{\mathrm{Eff}}} \mathrm{erg\ cm^3 s^{-1}}, \quad (7)$$

Table 2 gives values of Q^{Eff} and some other line parameters for three temperature-values. Using a denser temperature-grid, a very good numerical fit was obtained by $Q^{\mathrm{Eff}} = \mathrm{constant} + 16.6 \times (\log_{10} T - 6.96)^2$.

The contribution to the observed line flux from a plasma volume V with temperature T (in K) and emission measure $EM = n_e N_H V$ can then be computed by

$$f = EM \times P'/(4\pi d^2), \quad (8)$$

where the distance d of AB Dor is 15 pc (see Vilhu et al. 1998; Güdel et al. 2001).

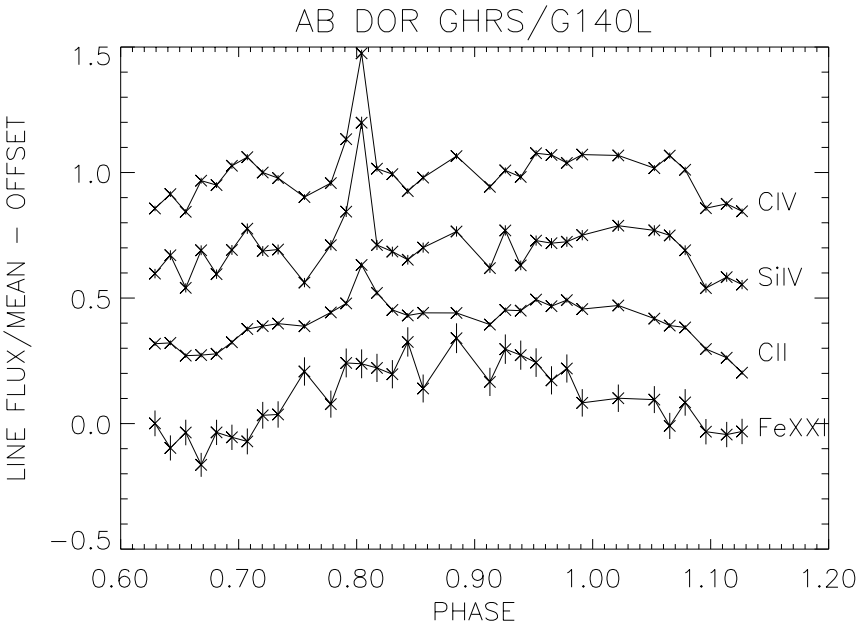

Fig. 3. Light curves of total intensities of selected lines marked in Fig. 2. The intensities are scaled with their mean values and shifted by 0, −0.3, −0.6 and −0.9 for CIV, SiIV, CII and FeXXI, respectively.

Using the observed FeXXI flux value from Table 1 and assuming solar iron abundance, this formula gives a value $(3.75-4.50)\times10^{52}$ cm^{-3} for the emission measure at 10^7 K depending on the ionisation fraction model (Ar-Ra or Ar-Ro). This value is in fact the *lower* limit if other temperatures contribute as well.

A multitemperature fit to the combined EUVE and ASCA data by Mewe et al. (1996) and 3-T fits to the XMM-Newton RGS2 and pn-CCD data (Güdel et al. 2001) give very similar total emission measures when integrated over temperature bins ($(7.5-9.5)\times10^{52}$ cm^{-2}) and a low iron abundance Fe/Fe$_\odot$ = 0.22. If such a low iron abundance is used to compute the emission measure for the FeXXI 1354 line, the resulting EM would be much higher ($(17-20)\times10^{52}$ cm^{-2}). Using a Bremsstrahlung continuum model to fit the EXOSAT (LE + ME) spectrum, Collier Cameron et al. (1988) arrived at a value of $(7-10)\times10^{52}$ cm^{-2} (scaling to a distance of 15 pc). All these values are plotted in Fig. 4 where 0.3 dex is assumed for the 1-T and 3-T fits of HST, XMM and EXOSAT while a more dense (0.1 dex) binning was used for the ASCA/EUVE data.

4. Discussion and conclusions

A striking feature of Fig. 4 is the similarity of the total emission measures obtained from different missions (EXOSAT, ASCA/EUVE, XMM-Newton) with different observing times, energy bands and spectral resolutions. The emission measure derived in the present paper from the FeXXI 1354.094 line deviates significantly from these, especially when the shallow line formation temperature range is considered.

Large variability would, of course, explain the discrepancy. During the present observations the variability was ±15 per cent and the 5.5 years of ROSAT monitoring did not resolve any pronounced variability in the soft X-ray flux (Kürster et al. 1997). However, we cannot exclude large variabilities in the shape of the differential emission measure curve, especially in the hot region where the FeXXI line is formed. By comparing the FeXXI 1354 line with other FeXXI lines in the EUVE-range, Linsky et al. (1998) concluded that there was large variability in Capella at 10^7 K. Using the *HST/STIS* Johnson et al. (2001) also concluded a large (factor of 5) variation of the FeXXI 1354 line in the G8 component of Capella. Hence, the variability may be the reason also to cause the unusual strength of the line in AB Dor, as well, but the parameter responsible for variations remains unsolved.

An explanation would be if the abundance at 10^7 K is higher and closer to the photospheric value (and possibly also variable), despite the ASCA/EUVE and XMM-Newton spectroscopic results. This would, however, require a rediscussion of these data to see whether such an abundance gradient is feasible. The problem is related to the inverse FIP-effect found by XMM-Newton in AB Dor (Güdel et al. 2001) and in HR 1099 (Brinkman et al. 2001). If the low-FIP elements (like iron) are deficient in the corona a natural question is where have they gone? One possibility is that they have been accelerated to the top of the corona (coronal loop apexes above 10^7 K) where the abundances are consequently larger. If such a temperature gradient is introduced to the fitting of XMM-Newton data the result would probably be a satisfactory FeXXI 1354 line but a too strong iron Kα line instead.

Marc Bos has been observing AB Dor frequently at his Mt Molehill observatory. The optical light curve between Sep. 8, 1995 – Jan. 8, 1996 showed a broad minimum between phases 0.2–0.6 (Bos 2000). Hence, although the HST observations were slightly outside this range (Feb. 5, 1996), it is probable that we observed AB Dor with HST during its maximum light, i.e. when the photospheric spot

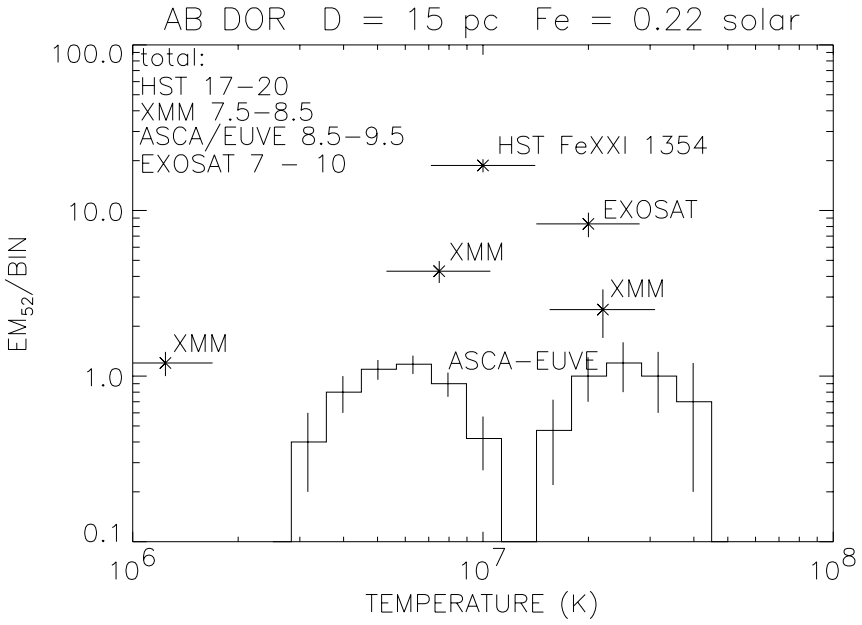

Fig. 4. Emission measures vs temperature (in units of 10^{52} cm^{-3} bin^{-1}, where bin = the temperature range of the emission measure in question) from different missions and observing periods are collected and compared. The total emission measures (summed over all temperature bins) are given in the upper-left corner.

complexes were situated behind the limb. If the small trend seen in Fig. 2 (broad maximum in the FeXXI 1354 light curve) is interpreted as due to the rotational modulation, this would mean that large active region and spot complexes were situated in opposite hemispheres.

During a flare Güdel et al. (2001) found the iron abundance to rise by a factor of 3. This could also partially solve the EM-problem discussed above, if the trend in Fig. 3 was part of a long-lasting flare (around the chromospheric-transition region flare visible at phase 0.8, see Fig. 3).

Although the spectral resolution of the G140L grating (resolving power = 2000) does not permit a detailed discussion of the line profiles, a few remarks concerning the line widths in Table 1 are worthwhile. All the lines are somewhat redshifted above the radial velocity of the star +30 km s^{-1}. The widths of the narrowest lines (Cl 1351.66 and OI 1355.60) are similar to those of SiIV 1400 and CIV 1549 (210–220 km s^{-1}). The width of this size can be explained by the combined rotational ($v \sin i = 100$ km s^{-1}) and instrumental (150 km s^{-1}) profiles. The larger width of the FeXXI line (325 km s^{-1}) cannot be explained by larger thermal velocity (90 km s^{-1} at 10^7 K) alone. It requires either larger rotational broadening or else an additional turbulent component of size 110 km s^{-1} (or both). Large rotation would be natural if an extended co-rotating corona (loops) is involved from the top of which the FeXXI line originates.

Acknowledgements. This work was performed with support from the Academy of Finland (OV) and Space Sesearch Organization of Netherlands (SRON) which is supported financially by NWO (RM). We are grateful to Diana Hannikainen for reading the manuscript and correcting our crude language. We thank Werner Curdt for providing the solar SUMER-spectrum and Marc Bos for information on his optical photometry.

Table 1. Observed parameters of selected lines in the FeXXI 1354 region (Fig. 2). The line flux is in units of 10^{-14} erg cm^{-2} s^{-1} and $FWHM$ in units of km s^{-1}.

λ (obs)	flux	$FWHM$	Identification
1351.99	1.25 ± 0.09	210 ± 20	Cl I 1351.66
1354.26	3.03 ± 0.3	325 ± 40	Fe XXI 1354.094
1355.98	1.18 ± 0.1	225 ± 30	O I 1355.60
2364.39	0.34 ± 0.05	255 ± 30	C I 1364.16
1371.66	1.04 ± 0.10	285 ± 40	O V 1371.29

Table 2. FeXXI λ1354.094 line parameters. The two values of $N_{\rm FeXXI}/N_{\rm Fe}$ and $Q^{\rm Eff}$ refer to the Ar-Ra (upper) and Ar-Ro (lower) ionization models.

$\log T$	6.8	7.0	7.2
$N_{\rm FeXXI}/N_{\rm Fe}$	0.0832	0.275	0.0214
- " -	0.0617	0.204	0.0158
$\bar{\Omega}(y)$	2.627e-2	1.990e-2	1.493e-2
Q	3.525	3.073	4.358
F	2.016	2.134	2.236
$Q^{\rm Eff}$	3.090	2.665	3.876
- " -	3.220	2.744	4.008

References

Aggarwal, K. M. 1991, ApJ, 77, 677
Arnaud, M., & Rothenflug, R. 1985, A&AS, 60, 425 (Ar-Ro)
Arnaud, M., & Raymond, J. 1992, ApJ, 395, 275 (Ar-Ra)
Anders, E., & Grevesse, N. 1989, Geochim. Cosmochim. Acta, 53, 197
Bos, M. 2000, private communication
Brandt, J. C., Heap, S. R., Beaver, E. A., et al. 2001, preprint
Brinkman, A. C., Behar, E., Güdel, M., et al. 2001, A&A, 365, L324
Collier Cameron, A., Bedford, D. K., Rucinski, S. M., Vilhu, O., & White, N. E. 1988, MNRAS, 231, 131
Curdt, W. 1998, private communication

Dere, K. P., Landi, E., Mason, H. E., Monsignori, Fossi, B. C., & Young, P. R. 1997, A&AS, 125, 149
Güdel, M., Audard, M., Briggs, K., et al. 2001, A&A, 365, L336
Innis, J. L., Thompson, K., Coates, D. W., & Evans, L. 1988, MNRAS, 235, 1411
Kürster, M., Schmitt, J. H. M. M., Cutispoto, G., & Dennerl, K. 1997, A&A, 320, 831
Linsky, J. L., Wood, B. E., Brown, A., & Osten, R. A. 1998, ApJ, 492, 767.
Mewe, R., GronenSchild, E. H. B. M., & van den Oord, G. H. J. 1985, A&AS, 62, 197
Mewe, R., Kaastra, J. S., White, S. M., & Pallavicini, R. 1996, A&A, 315, 170
Pagano, I., Linsky, J. L., Carkner, L., et al. 2000, ApJ, 532, 497
Robinson, R. D., Airapetian, V. S., Maran, S. P., & Karpenter, K. G. 1996, ApJ, 469, 872
Rucinski, S. M., Mewe, R., Kaastra, J. S., Vilhu, O., & White, S.M. 1995, ApJ, 449, 900
Vilhu, O., Gustafsson, B., & Edwardsson, B. 1987, ApJ, 320, 850
Vilhu, O., Tsuru, T., Collier Cameron, A., et al. 1993, A&A, 278, 467
Vilhu, O., Muhli, P., Huovelin, J., et al. 1998, AJ, 115, 1610
Wilhelm, K., Woods, T. N., Schühle, U., et al. 1999, A&A, 352, 321